

Imaging and identification of atomic planes of cleaved $\text{Bi}_2\text{Sr}_2\text{CaCu}_2\text{O}_{8+\delta}$ by high resolution scanning tunneling microscopy

S. H. Pan, E. W. Hudson, J. Ma, and J. C. Davis^{a)}

Department of Physics, University of California, Berkeley, California 94720

(Received 17 March 1998; accepted for publication 1 May 1998)

Imaging of the surface of a cleaved $\text{Bi}_2\text{Sr}_2\text{CaCu}_2\text{O}_{8+\delta}$ (BSCCO) single crystal with a scanning tunneling microscope reveals a series of repeating terraces, whose separations are then used to identify the atomic planes which are exposed. On each of the exposed planes, the incommensurate modulation is also clearly resolved with atomic resolution. The measured separations between the terraces lead to the deduction that any atomic layer can be exposed by mechanical cleavage of BSCCO. We, therefore, suggest that the identity of atomic planes, and the direction of tunneling, should always be taken into consideration when interpreting tunneling spectra obtained on such cleaved BSCCO crystals. © 1998 American Institute of Physics. [S0003-6951(98)00727-X]

Electron tunneling is a very widely used technique in the study of the electronic properties of materials. Numerous demonstrations of the success of this technique are available.¹ However, its application to high- T_c superconductors has not been quite as successful as one might expect. One reason for this is that the high- T_c cuprates are very complex, both in their mechanical and electronic structure. In tunneling spectroscopy, one has the standard considerations of tunnel junction configuration, and of surface condition of the tunneling electrodes. When interpreting tunneling results obtained from high- T_c materials, however, one should also consider onto which atomic planes, and in which directions, the tunneling measurement is performed. This is relevant because the superconducting coherence length is so short in these materials² that the electron density of states (DOS) is different for different atomic planes.³ Furthermore, because of the highly anisotropic properties of the high- T_c cuprates, the energy dependence of the DOS is also a strong function of the \mathbf{k} vector.³

With $\text{Bi}_2\text{Sr}_2\text{CaCu}_2\text{O}_{8+\delta}$ (BSCCO) it has often been assumed that when a single crystal is cleaved along the a - b direction the exposed surface is the BiO plane, and that the tunneling process occurs perpendicularly into this atomic plane. However, in this letter, we demonstrate by high resolution scanning tunneling microscopy (STM), that these conditions do not necessarily always occur.

In this study we use a home-built very low temperature STM,⁴ which operates in cryogenic ultrahigh vacuum (UHV). Calibration of the scanner is carried out by using a Au, $\langle 111 \rangle$ oriented, single crystal as the sample. Atomic resolution imaging and stable spectroscopy are verified on this crystal. Then, the piezosensitivity in the direction perpendicular to the sample surface is calibrated against the atomic step sizes seen on the Au $\langle 111 \rangle$ surface to an accuracy of 0.01 nm.

The BSCCO single crystals used in this study were grown using a flux growth method based on standard techniques described elsewhere,⁵ and are reoxygenated just prior

to imaging. The onset of the superconducting transition is measured to be at 83 K, with a transition width of 9 K. The crystal is introduced into the cryogenic UHV from room temperature and cooled to 4.2 K. It is cleaved by a mechanical cleaver and then inserted into the STM head, which is already at 4.2 K.

A topographic image of the surface achieved after one particular cleavage of a BSCCO crystal is displayed in Fig. 1. It shows a series of 16 terraces stepping down from the top right to the bottom left corner. Every fourth terrace is broader than the others, and the broad terraces repeat twice in each unit cell of the crystal (as determined below). There is an incommensurate modulation (which runs throughout the bulk BSCCO crystal⁶⁻⁹) which appears as a sinuous structure running along the \mathbf{b} axis.¹⁰⁻¹⁴ It displaces atoms from their crystal sites along all three directions. We clearly image this modulation on all terraces, and can follow it from one terrace to the next across step edges throughout the entire field of view. Figure 2, which is a zoomed-in view of one of the broad terraces, shows the supermodulation with

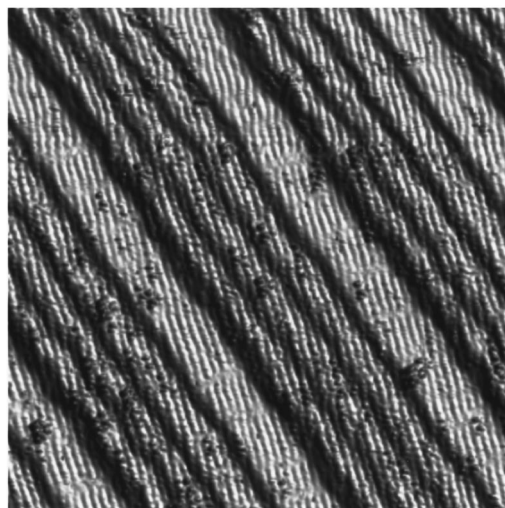


FIG. 1. Constant current image (145 nm \times 145 nm) of the surface of a cleaved BSCCO crystal, showing the supermodulation running along multiple terraces. Imaged at $T=4.2$ K ($I=4$ pA, $V_{\text{sample}}=+900$ mV).

^{a)}Electronic mail: jcdavis@socrates.berkeley.edu

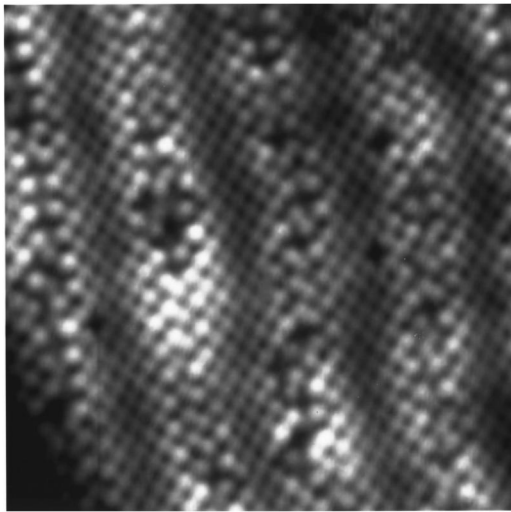


FIG. 2. High resolution image (100 Å×100 Å) on one of the broad terraces, showing dislocations and the supermodulation with atomic resolution. (Raw data, imaged at $T=4.2$ K, $I=4$ pA, $V_{\text{sample}}=+900$ mV).

atomic resolution. The dark area in the bottom left hand corner is the fall off of the surface at the step edge. In addition to the supermodulation, there are several different types of atomic dislocations at the crest of the supermodulation which are clearly resolved. They appear as an additional displacement of atoms beyond that due to the supermodulation. We do not know the origin of these structural features, although they are observed on almost all cleaved BSCCO surfaces which we have studied. Careful examination showed that, along with the supermodulation, these dislocations exist on all of the atomic planes shown in Fig. 1.

Figure 3 is a schematic diagram of the unit cell of the BSCCO (2212) crystal, with the distances between the planes shown as determined by x-ray diffraction.¹⁵ We see that there are seven possible atomic layers which could be exposed in each half-unit cell, namely, the BiO, SrO, CuO₂, Ca, CuO₂, SrO, and BiO planes. To identify which atomic planes are exposed in Fig. 1, we first make a histogram of the topographic data (the measured height of each point on the surface). This results in a series of peaks in the distribution, each peak corresponding to a particular terrace. These peaks are much wider than the resolution of the STM (1 pm) because of the smearing effect of the supermodulation. We

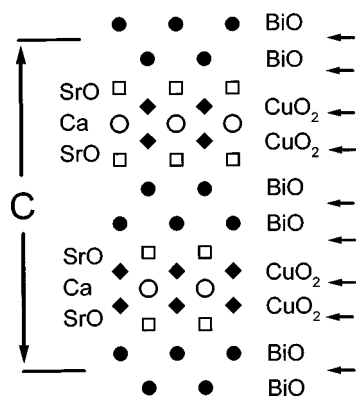


FIG. 3. Schematic diagram, showing the unit cell of BSCCO (2212). The unit cell height is denoted by C. The arrows, at right, indicate the identified cleavage planes.

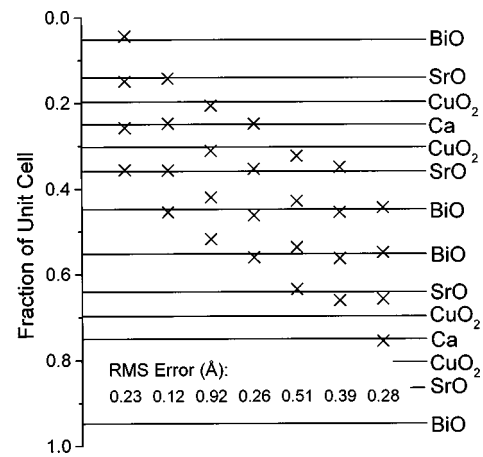


FIG. 4. Seven possible identifications of the crystal terraces seen in Fig. 1. Each column of X's corresponds to the position of a broad terrace and the three terraces below it, whose separations are measured by STM. The rms error from the least squares fit for each possibility is indicated below its column.

determine the height of each terrace from the center of the associated peak in the distribution. The z distances between each pair of the five broad terraces is 1.570(2) nm, 1.554(1) nm, 1.554(1) nm, and 1.529(3) nm, as determined by the STM. The average is 1.552 ± 0.02 nm, which agrees well with the known size of the half-unit cell length of 1.545 nm.^{6,15}

To further identify the exposed atomic layers, the measured terrace separations are scaled to fractions of a unit cell and a least squares fit to the separations as determined by x-ray diffraction is performed. Because of symmetry, each set of terraces (one broad and the three below it) has seven possibilities for a fit to the crystal structure (as shown in Fig. 4). The standard errors for the best fits are comparable, and thus, the fit alone is not sufficient to determine which possibility represents the actual cleavage. However, since the longest and the weakest bonds are between two adjacent BiO planes,^{10,16} we propose that the widest terrace is the BiO layer. This assumption immediately leads to the identification of the exposed atomic planes as BiO, SrO, Ca, and SrO in each half-unit cell (the left-most set displayed in Fig. 4). It should be noted that in constant current mode topographic images, the terrace ‘‘height’’ depends not only on the physical separation of the atomic layers but on their DOS as well. Since, in the above analysis, no account was taken of variation of the DOS on different atomic planes, the error of the fit for the suggested cleavage is not unreasonable.

Even without the above assumption, as can be seen in Fig. 4, between the crystal surface we observed, and its complementary surface (on the piece cleaved off), all atomic planes were exposed. Thus, a very important implication can still be deduced—when a tunnel junction is made on a mechanically cleaved surface, it is possible that the tunneling is performed onto any atomic plane, or onto multiple planes of different types. Furthermore, the tunnel current may be not only perpendicular to the atomic planes but also consist of contributions into the plane (i.e., a - b direction) through step edges.

In conclusion, we have imaged surfaces of multiple atomic layers of a cleaved BSCCO crystal. Based on the

assumption that the broadest terraces are BiO layers, we were able to identify the other atomic layers which were exposed. The supermodulation is imaged with atomic resolution and shown to pass from each terrace to the next without interruption. The important implication drawn from this work is that a BSCCO single crystal, mechanically cleaved along *a-b* direction, may leave a surface with any atomic plane exposed, possibly with multiple terraces and step edges. Thus, the interpretation of tunneling results must take into consideration the identity of the atomic planes and the directions in which the measurement is performed.

The authors are grateful to G. Yang for providing us with the BSCCO (2212) single crystal samples used in this study. The authors thank A.L. de Lozanne and R.E. Packard for valuable conversations. This work is supported by the NSF under Grant No. DMR 94-58015 and by the D&L Packard Foundation.

¹E. L. Wolf, *Principles of Electron Tunneling Spectroscopy*, International Series of Monographs on Physics (Oxford University Press, New York, 1985), p. 71.

²For a review, see, e.g., M. B. Salamon, in *Physical Properties of High Temperature Superconductors I*, edited by D. M. Ginsberg (World Scientific, Singapore, 1989), p. 39.

³D. J. Singh and W. E. Pickett, *Phys. Rev. B* **51**, 3128 (1995).

⁴S. H. Pan, E. W. Hudson, and J. C. Davis (unpublished).

⁵G. Yang, S. Sutton, P. Shang, C. E. Gough, and J. S. Abell, *IEEE Trans. Appl. Supercond.* **3**, 1663 (1993).

⁶S. A. Sunshine, T. Siegrist, L. F. Schneemeyer, D. W. Murphy, R. J. Cava, B. Batlogg, R. B. van Dover, R. M. Fleming, S. H. Glarum, S. Nakahara, R. Farrow, J. J. Krajewski, S. M. Zahurak, J. V. Waszczak, J. H. Marshall, P. Marsh, L. W. Rupp, Jr., and W. F. Peck, *Phys. Rev. B* **38**, 893 (1988).

⁷Y. Gao, P. Lee, P. Coppens, M. A. Subramanian, and A. W. Sleight, *Science* **241**, 954 (1988).

⁸H. Budin, O. Eibl, P. Pongratz, and P. Skalicky, *Physica C* **207**, 208 (1993).

⁹S. Horiuchi and E. Takayama-Muromachi, in *Bismuth-Based High-Temperature Superconductors*, edited by H. Maeda and K. Togano (Marcel Dekker, New York, 1996), Chap. 2.

¹⁰M. D. Kirk, J. Nogami, A. A. Baski, D. B. Mitzi, A. Kapitulnik, T. H. Geballe, and C. F. Quate, *Science* **242**, 1673 (1988).

¹¹C. K. Shih, R. M. Feenstra, J. R. Kirtley, and G. V. Chandrashekhar, *Phys. Rev. B* **40**, 2682 (1989).

¹²Ch. Renner and Ø. Fischer, *Phys. Rev. B* **51**, 9208 (1995).

¹³H. Murakami and R. Aoki, *Proc. SPIE* **2696**, 384 (1996).

¹⁴Ali Yazdani (private communication).

¹⁵M. A. Subramanian, C. C. Torardi, J. C. Calabrese, J. Gopalakrishnan, K. J. Morrissey, T. R. Askew, R. B. Flippen, U. Chowdhry, and A. W. Sleight, *Science* **239**, 1015 (1988).

¹⁶P. A. P. Lindberg, Z. X. Shen, B. O. Wells, D. Dessau, D. B. Mitzi, I. Lindau, W. E. Spicer, and A. Kapitulnik, *Phys. Rev. B* **39**, 2890 (1989).